Identification of two light-induced charge states of the oxygen vacancy in single-crystalline rutile TiO_2

F. D. Brandão,[1] M. V. B. Pinheiro,[1] G. M. Ribeiro,[1] G. Medeiros-Ribeiro,[2] and K. Krambrock[1,*]
[1]*Departamento de Física, Universidade Federal de Minas Gerais, CP 702, 30.123-970 Belo Horizonte, MG, Brazil*
[2]*Hewlett-Packard Laboratories, Palo Alto, California 94304, USA*

(Received 18 July 2009; revised manuscript received 8 October 2009; published 22 December 2009)

The nonstoichiometry of the main structural phase of TiO_2 (rutile) and its natural *n*-type conductivity is due to oxygen deficiency, which has been explained in terms of native defects, i.e., oxygen vacancies and titanium interstitials. While the latter has been unambiguously identified by electron paramagnetic resonance (EPR) and attributed to a shallow donor, the oxygen vacancy lacks such identification, in fact, any identification at all. In this work, two charge states of the oxygen vacancy, i.e., the singly V_O^+ and doubly V_O^0 occupied charge states with $S=0.5$ and $S=1$, respectively, are identified by EPR under blue light excitation in fully oxidized TiO_2 (rutile). It is shown that the vacancy is a very shallow donor (2.8 meV) and that both charge states suffer different strong lattice relaxations depending on charge.

DOI: 10.1103/PhysRevB.80.235204 PACS number(s): 71.20.Nr, 76.30.Da, 71.55.Ht

I. INTRODUCTION

Titanium dioxide (TiO_2) is actually one of the most studied materials in nanotechnology with important applications in heterogeneous photocatalysis,[1] hydrolysis of water,[2] solar cells,[3] and gas sensors[4] and recently as one of the materials utilized in devices embodying the fourth passive electronic element, the memristor,[5] as well as in resistive switches with nonvolatile memory applications.[6] Nonstoichiometric TiO_{2-x} exhibits *n*-type conductivity, which is caused by oxygen vacancies and/or titanium interstitial defects. For most applications, a deep understanding of the intrinsic defects is crucial because these may act as charge trapping centers or may induce light absorption bands in the visible spectral range. Defects are important for photocatalytic reactions because of transferred electronic charge. A defect-free TiO_2 is not photocatalytic.[7] One of the most controversially discussed intrinsic defects in TiO_2 is the oxygen vacancy. Although recent theoretical calculations investigated the electronic structure of the oxygen vacancy in the surface due to its important role in photocatalysis, not much has been done for it in bulk rutile [Refs. 7(a) and 7(b), and references therein]. On surfaces, a gap state observed at about ~0.85 eV below the conduction band has been associated for a long time to bridging oxygen vacancies,[8] however, recently is was shown that the surface vacancy can be removed without affecting the gap state, i.e., the gap state is associated with a Ti interstitial defect localized just below the surface.[7(b)] Recent first principles studies of point defects in reduced bulk rutile found that the oxygen vacancy does not introduce gap states, whereas the Ti interstitial has a gap state of about 0.2 eV below the conduction band.[9] Given of the importance of this defect in understanding of electronic transport phenomena, it is of utmost importance to identify its signatures with an appropriate technique.

Intrinsic defects in reduced and reoxidized TiO_2 (rutile) have been studied before by electron paramagnetic resonance (EPR).[10] All observed intrinsic defects have been attributed to Ti interstitial defects and pairs of them. No evidence was found for the existence of paramagnetic states of the oxygen vacancy. Recently, photo-induced paramagnetic defects in TiO_2 (rutile) were studied by electron paramagnetic resonance.[11] It was proposed that two charge states of the oxygen vacancy can be occupied by below (blue) and above band gap light at low temperatures in oxidized TiO_2 (rutile) that contained small amount of transition metal impurities. However, a clear identification of the oxygen vacancy was not given, i.e., symmetry in the different charge states, their possible distortions and numbers of magnetically inequivalent sites. Photo-induced paramagnetic charge states in TiO_2 have also been observed before, however, without identification of the specimen.[12]

In this work, the two charge states of the singly and doubly occupied charge states of the oxygen vacancy have been identified by electron paramagnetic resonance at low temperatures under below and above band gap illumination. Resistivity measurements under the same conditions have been also performed. Detailed analysis of the EPR angular dependencies allow for the clear identification of the oxygen vacancy and show that the vacancy suffers strong lattice relaxation depending on charge.

II. EXPERIMENTAL

The EPR technique is a powerful method for structural analysis of point defects in solids which may control their optical and electrical properties even in concentrations of a few ppm. In general, the local site, the local symmetry, spin state, hyperfine and sometimes the superhyperfine interactions of the paramagnetic defect can be obtained from the analysis of the EPR spectra within the spin Hamiltonian formalism.[15] From that information a full description of the paramagnetic states of the defect is possible.

EPR spectra were recorded on a homemade spectrometer which includes a 500 mW klystron (Varian), a commercial resonance cavity (Bruker) with optical access perpendicular to the cavity axis, an electromagnet (Varian) with maximum field amplitudes of 800 mT and a He flux cryosystem (Oxford) for low-temperature measurements. For the angular variations the sample holder was rotated automatically by a

 ©2009 The American Physical Society

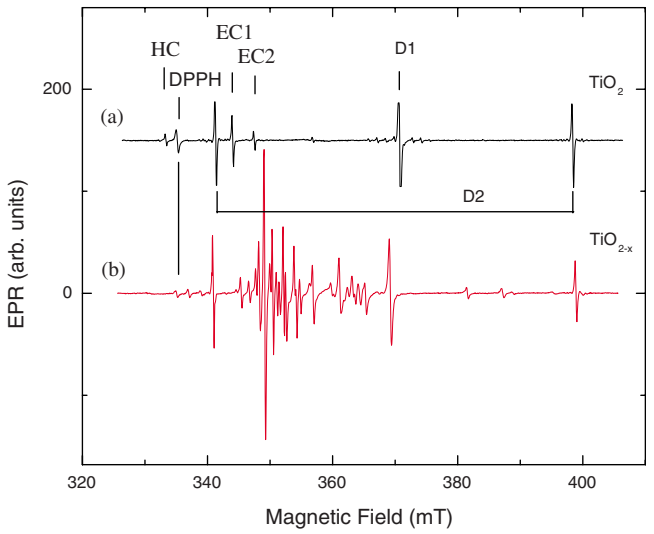

FIG. 1. (Color online) EPR spectra measured at 25 K with microwave frequency of 9.40 GHz for $B\|[001]$ in (a) oxidized TiO_2 under blue light (470 nm, 5 mW) (black line, the intensity of the $S=0.5$ line is slightly cut) and (b) reduced TiO_2 in dark (red line). It should be noted that before illumination no EPR spectrum was observed in the oxidized sample and that the EPR lines in the reduced sample are not affected by the illumination.

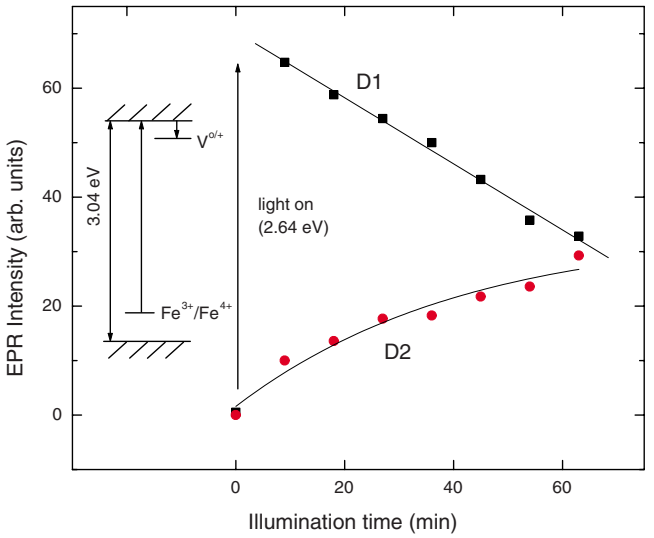

FIG. 2. (Color online) EPR signal intensities of paramagnetic defect D1 (EPR line centered at 369 mT, black solid squares) and D2 (EPR line centered at 341 mT, red solid circles) as a function of illumination time (470 nm, 5 mW) measured at 25 K upon illumination in the oxidized TiO_2 sample.

goniometer. Microwave frequency was stabilized by an automatic frequency control (AFC) and measured with high precision frequency meter (PTS). For g-factor calibration the stable radical 2,2-diphenyl-1-picrylhydrazyl has been used ($g=2.0037$). Spectra were recorded using 100 kHz field modulation technique and Lock-In technique (EG & G Princeton). For the illumination experiments different commercial LEDs were applied.

Two synthetic oxidized TiO_2 (rutile) single crystals from MTI (USA) and CRYSTEC (Germany) were investigated by EPR. Polished samples were cut to plates of $3\times3\times1$ mm^3 with faces oriented along [110], [1$\bar{1}$0], and [001]. Samples from the same substrate were partially reduced at 1000 °C for two hours in ultrahigh vacuum. Before reduction treatment, the samples were slightly yellow, whereas after they turned medium blue with strongly reduced electrical resistance.

III. EXPERIMENTAL RESULTS

In dark, oxidized MTI crystals show low concentrations of paramagnetic substitutional Fe^{3+} impurities (~few ppm) on Ti sites.[13] Under UV light (375 nm, 16 mW) and also under blue light (470 nm, 5 mW), and at low temperatures (15–30 K), at least five different paramagnetic defects are observed, which are partially thermally persistent at these temperatures. Figure 1 shows the X-band EPR spectra for the (a) oxidized and (b) reduced MTI sample measured at 25 K with microwave frequency of 9.40 GHz and 60 dB of full klystron power, i.e., with about 0.1 μW, measured with a solid state microwave amplifier in the detection arm of the microwave bridge.

While the EPR spectrum of the oxidized sample was measured after the sample was illuminated with blue light for 30 min., the spectrum of the reduced sample was unchanged upon illumination. The EPR lines marked as D1 and D2 belong to two charge states of the same defect (as shown below), which were attributed recently to the oxygen vacancies in their singly and doubly occupied charge states, namely, V_O^+ and V_O^0, respectively.[11] However, we will refer to them as the charge states of oxygen vacancy only after its full identification. In addition to that, other paramagnetic defects are observed after illumination of the oxidized sample: two electron centers EC1 and EC2, $g<g_e$, and one hole center HC1 with $g>g_e$, in addition to a light-induced Ni center (at lower magnetic fields, not shown in the figure).[14]

The EPR spectra of all paramagnetic centers are strongly affected by temperature, light and microwave power. The EPR spectra in the reduced sample do not change under illumination with UV or blue light. In the reduced samples apart from dominant EPR spectra of interstitial Ti^{3+} and pairs of them,[10] also the oxygen vacancy in both its charge states was observed, in addition to other minority paramagnetic centers.[11] In the present work we will focus on the EPR lines in the oxidized sample marked as D1 and D2, mentioned before, and compare to the same lines in the reduced sample.

The EPR signals D1 and D2 are correlated with each other and the relationship between the intensity of EPR signals are presented in Fig. 2. Before light exposure no EPR signal is observed in the 320 to 400 mT magnetic field range when the field is along the [001] crystal orientation. After 10 min of blue light or UV illumination an intense EPR line labeled as D1 at 369 mT and two less intense EPR lines labeled as D2 are observed at 341 mT and 396 mT for [001]. Under continuous light irradiation EPR signal D1 becomes less intense; meanwhile, the intensity of the two EPR signals D2 grow until saturation which is reached after about two

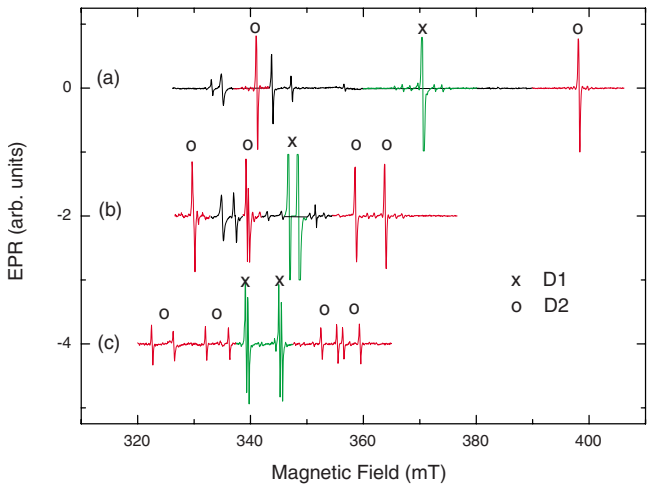

FIG. 3. (Color online) EPR spectra of paramagnetic defect D1 (green, marked by *x*) and D2 (red, marked by o) measured at 20 K with microwave frequency of 9.40 GHz and microwave power of 0.1 μW in oxidized TiO_2 under blue light for (a) $B\|[001]$, (b) $B\|[110]$ and (c) an arbitrary orientation in (001) plane.

hours of light illumination (see Fig. 2). When the light is turned off at 20 K, the EPR signals are persistent. However, for temperatures of about 30 K, first the two EPR lines D2 decrease with increase of the line D1. After complete disappearance of the lines D2, EPR line D1 is still measurable for about one hour. From these illumination experiments at low temperature in the same oxidized sample we conclude that both the EPR signals are correlated, i.e., originate from the same defect in two charge states denoted as D1 and D2, i.e., line D1, a singlet line, belongs to the spin $S=0.5$ state with one electron and the doublet D2 belongs to the spin $S=1.0$ state with two electrons.

Figure 3 shows some EPR spectra in the fully oxidized sample under blue light illumination for three different orientations of the magnetic field with respect to the crystal axes. In the figure, the green part of the spectra corresponds to the EPR line D1, the red to the two EPR lines D2. From the figure it can be noticed that for both charge states in the [001] direction only one magnetically inequivalent site is observed, for the [110] and $[1\bar{1}0]$ and two inequivalent sites (this is also true for the [100] and [010] directions) and for arbitrary orientation four inequivalent sites.

Figures 4(a) and 4(b) show the angular dependencies of the EPR spectra related with D1 and D2, respectively. In the figure the symbols represent the EPR line positions and the solid lines the fitted angular dependencies.

IV. STRUCTURAL ANALYSIS

The EPR angular dependencies were analyzed by using the following spin Hamiltonian:[15]

$$H = \beta \mathbf{S} g \mathbf{B} + \mathbf{S} D \mathbf{S} + \Sigma_i \mathbf{S} A \mathbf{I}_i. \quad (1)$$

The first term in Eq. (1) corresponds to the electronic Zeeman interaction, the second to the electronic fine structure interaction for ($S \geq 1$) and the third to the hyperfine or

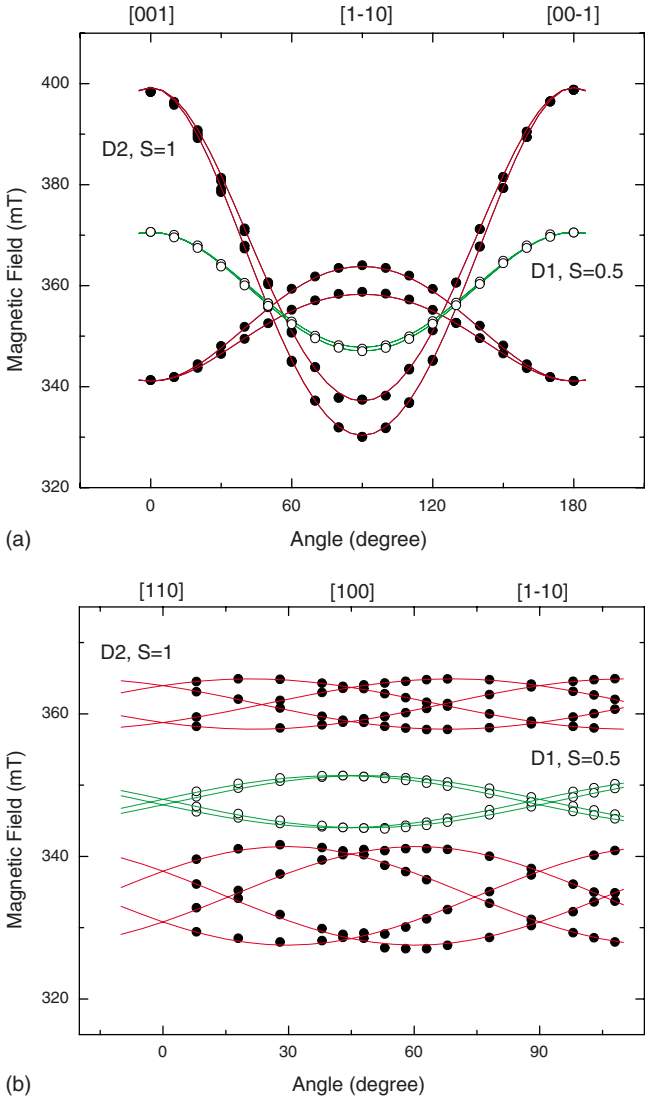

FIG. 4. (Color online) EPR angular dependencies in the (a) (110) and (b) (001) planes measured at 20 K under blue light excitation of D1 ($S=0.5$) and D2 ($S=1$). Dots correspond to EPR line positions and solid lines to calculated line positions.

superhyperfine (shf) interaction. The symbols have their usual meaning.[15] Small misalignments of the sample have been taken into account. The parameters of the spin Hamiltonian were evaluated by fitting simultaneously all line positions in two perpendicular crystal planes (solid lines in Fig. 4), the (110) and (001) plane, using exact diagonalization of the spin Hamiltonian of Eq. (1) for tetragonal symmetry. In total, 160 resonance line positions were taken into account in the analysis. The spin Hamiltonian parameters are listed in Table I, i.e., the principal values of the interaction tensors and their orientations. For the EPR line marked as D1 ($S=0.5$) only the first term of Eq. (1), whereas for the two EPR lines marked as D2 ($S=1.0$) also the second term was taken into account. It should be noted that only the relative sign of the electronic fine structure term was determined because of strong microwave saturation effects at lower temperatures. A distorted axial symmetry is determined, i.e., the *g* and *D* tensors show three different principal values. For pure axial

TABLE I. (Color online) Spin Hamiltonian parameters, principal values and orientations of the interaction tensors of the oxygen vacancy in TiO_2 (rutile) in its two charge state V_O^+ and V_O^0 with $S=0.5$ and $S=1$, respectively. D is given in MHz. Spin Hamiltonian parameters of defects A, X, and W from Ref. 10. The angles describe the orientation of the principal axes of the g and D tensors in relation to the [001] and [110] axes: Θ polar angle and φ azimuthal angle.

		Z	X	Y	Principal axes of tensors
V_O^+	g	1.8132(4)	1.9526(1)	1.9117(1)	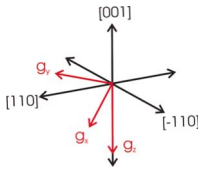
	(Θ/φ)	180/0	90/49	90/319	
V_O^0	g	1.8147(4)	1.949(2)	1.9093(1)	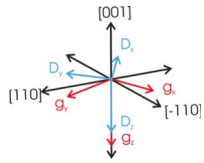
	(Θ/φ)	180/0	90/105	90/15	
	$\lvert D\rvert$	484.3(6)	−165.2(6)	−319.1(6)	
	(Θ/φ)	180/0	90/221	90/311	
A(C)	g	1.9414	1.9780	1.9746	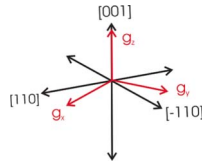
	(Θ/φ)	0/0	90/19	90/109	
X	g	1.9509	1.9846	1.9802	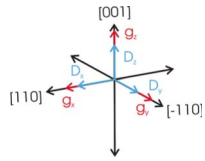
	(Θ/φ)	0/0	90/0	90/90	
	$\lvert D\rvert$	57.0	30.0	27.0	
	(Θ/φ)	0/0	90/0	90/90	
W	g	1.791	2.053	1.835	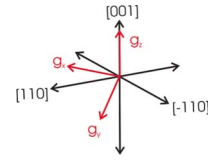
	(Θ/φ)	0/0	90/309.5	90/49.5	

symmetry only two independent principal values are expected.

The TiO_2 structure in the rutile phase has tetragonal space group $P4_2/mmm$ with lattice parameters a and c given by 4.584 and 2.959 Å, respectively, and two molecules per unit cell ($Z=2$).[8] According to this space group, the two Ti atoms occupy a sites, the four oxygen atoms f sites and the four empty octahedral interstitial positions c sites. The local point symmetries of these sites are mmm, mm, and $2/m$, respectively.[16] Therefore, the observed EPR spectra and their splitting are in accordance either with an intrinsic defect on the interstitial position or with a defect on the oxygen site position, i.e., one magnetically inequivalent site for $B\|[001]$, two for $B\|[110]$ and [100], and four for arbitrary orientations.

Intrinsic defects as the isolated Ti interstitials and pair defects of them have been studied before[10] in reduced bulk single crystalline rutile (TiO_2) by EPR. Isolated Ti interstitials have been denoted A or C defects—A for low concentrations and C for high concentrations—Ti pair defects with $S=1.0$ as X and Ti pair defects with $S=0.5$ as W. None of these defects are consistent with the two observed charge states of the same intrinsic defect in our study, although the W defect shows similar EPR angular dependencies and symmetry of the principal axes of the g tensor compared with the EPR line D1 investigated in this work. The principal axes of its g tensor are along the [001] direction and two others in the (001) plane with small deviations of about ±4° of the [100] and [010] axes. Because of these deviations, the authors excluded a simple point defect or simple defect complex,[10] which is the case for most cases. In the reduced crystals the X and W defects do not show any correlation with each other. The X defect with spin $S=1.0$, which was associated to a pair of Ti interstitials[10] has its principal g and D tensor axes along the [001] crystal axis and the two diagonals in the (001) plane, i.e., the [110] and equivalent directions. For the $S=1.0$ state of the oxygen vacancy studied in this work, the principal axes of the g and D tensors are along [001] direction and two in the (001) plane with deviations from the diagonals by 15° and 49°, respectively. In addition, the magnitudes of the distortions and interactions for the observed defect in this work, in its two charge states, are much bigger than Ti related defects (A, C, and X). Therefore, we attribute the observed defect to a substitutional defect on

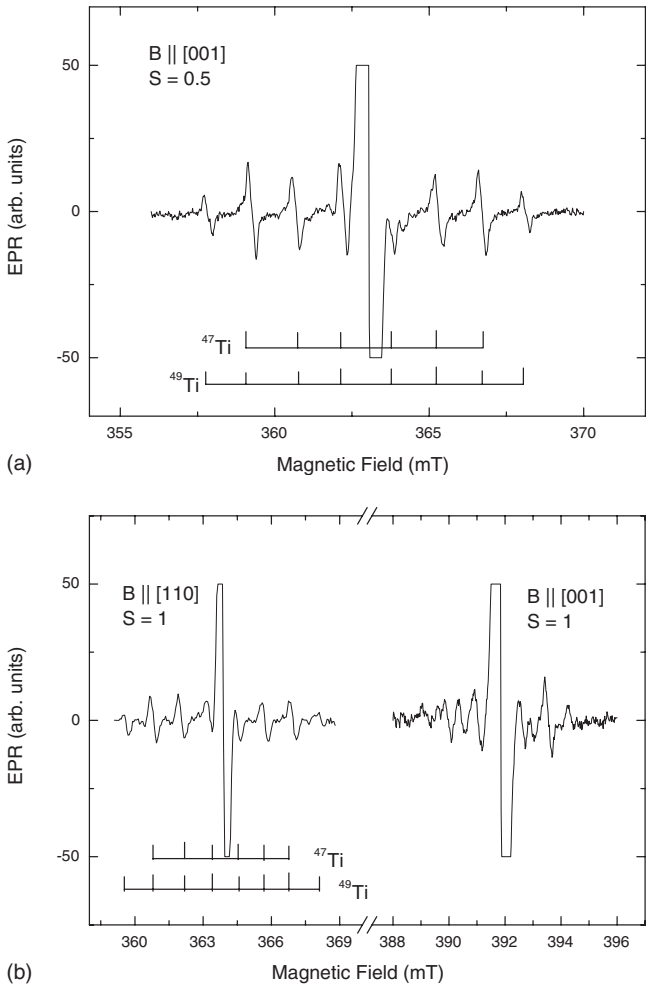

FIG. 5. EPR spectra of oxygen vacancy in charge states (a) V_O^+ (S=0.5) for $B\|[001]$ and (b) V_O^0 (S=1) for $B\|[110]$ and [001] showing shf interaction due to the two Ti isotopes ^{47}Ti (I=5/2, 7.4%) and ^{49}Ti (I=7/2, 5.4%).

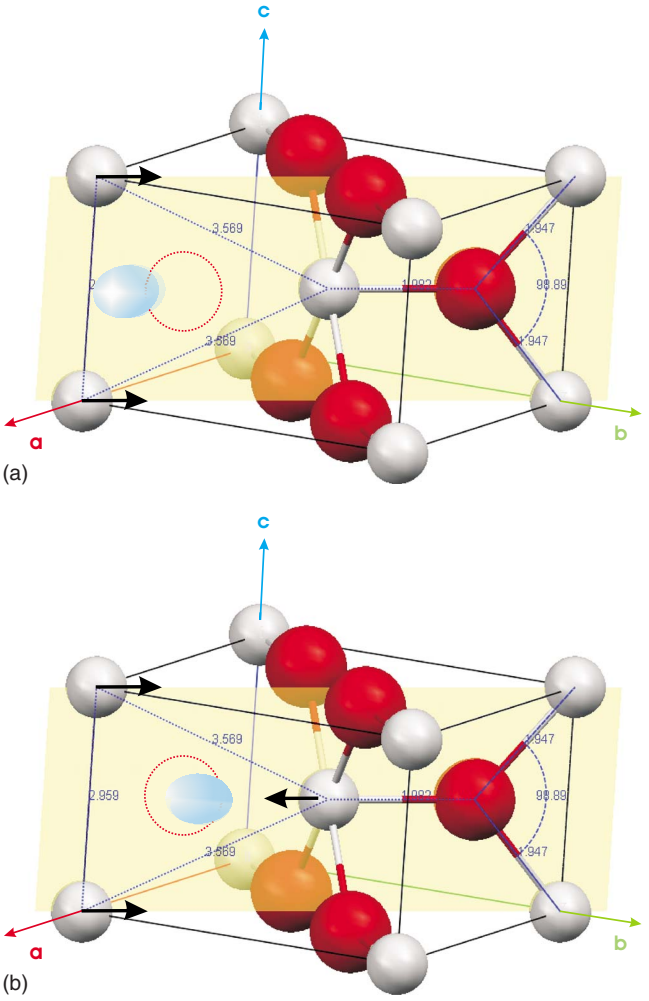

FIG. 6. (Color online) Local symmetry around the oxygen vacancy in the TiO_2 structure (rutile) in the two charge states (a) V_O^+ (S=0.5) and (b) V_O^0 (S=1.0). Ti and O atoms are shown as gray and red circles, respectively. Relaxed position of the vacancy is indicated by the positions of the bluish ellipsoids. Arrows indicate possible relaxations of the Ti neighbors.

the oxygen site of the rutile structure. The most probable defect model that satisfy all the observations is the oxygen vacancy in two charge states, i.e., the singly occupied denoted as D1 with spin S=0.5, V_O^+, and the doubly occupied denoted as D2 with spin S=1.0, V_O^0.

The EPR lines due to the oxygen vacancy show some additional line splitting. Figure 5(a) shows such splitting for the magnetic field along the [001] direction for V_O^+. In the figure the EPR line shows eight equidistant lines with distance of 1.4 mT, which corresponds to a shf interaction of 39.1 MHz. The intensity ratios of the lines are exactly what are expected for the hyperfine or superhyperfine interaction with the Ti isotopes with nuclear spin I: ^{47}Ti (I=5/2, 7.4%) and ^{49}Ti (I=7/2, 5.4%). When rotating the sample in the (110) plane the magnitude of the shf interaction of V_O^+ is reduced and the lines are split due to at least two inequivalent Ti ions. A detailed analysis of the shf interaction was not possible because of line superpositions. Also for the V_O^0 charge state of the oxygen vacancy shf splitting is observed (Fig. 5(b)). For the high-field EPR line of the V_O^0 the distance between the shf lines is much less with about 0.5 mT, which corresponds to a shf interaction of 14.0 MHz for the [001] direction about three times less when compared to the splitting for V_O^+ in the same direction. In this orientation the line shape is asymmetric indicating that at least two inequivalent Ti ions are involved. For the [110] direction (Fig. 5(b)) the shf interaction of the all Ti neighbors are equivalent for V_O^0 with similar magnitude as for V_O^+ in the [110] direction, i.e., about 1.3 mT, which corresponds to 36.3 MHz.

Figure 6 represents the rutile unit cell containing an oxygen vacancy with its first three Ti neighbors and some of its oxygen neighbors. The distances correspond to the ideal rutile structure.[8] The orientations of the principal axes of the g tensors of the two charge states of the oxygen vacancy are indicated as ellipsoids at relaxed positions in Figs. 6(a) and 6(b) for V_O^+ and V_O^0, respectively.

From the observation of the different Ti neighbor shf interactions of the oxygen vacancy in the two crystal directions [001] and [1$\bar{1}$0] we can conclude that the oxygen vacancy suffers strong relaxations depending on the charge state. For the oxygen vacancy shf interaction from three first neighbors

Ti ions are expected; one at the center of the unit cell and other two at the corners. For the positive charge state of the vacancy we observed the strongest interaction along the [001] direction. For other directions we detected a reduced and nonequivalent shf interaction. These results imply that the vacancy has strongest overlap with the two Ti neighbors along the [001] direction. From that we conclude that either the vacancy is relaxed toward the Ti neighbors on the [001] direction or the two Ti neighbors relaxes toward the vacancy [see Fig. 6(a)]. On the other hand, for the neutral charge state of the oxygen vacancy the strongest shf interaction is observed along the diagonal $[1\bar{1}0]$ direction and a much smaller and more asymmetrical one along the [001]. In this case the oxygen vacancy has to relax toward a central position between the first three Ti neighbor ions, i.e., an equidistant position. From purely geometrical considerations this implies relaxation of approximately 20% from its original position [see Fig. 6(b)].

These relaxations are indicated in the Fig. 6 by the positions of the ellipsoids, which results from the interpretation of different shf interactions for both charge states. Both show relaxation along the $[1\bar{1}0]$ direction, however, in opposite directions, i.e., the positive charged vacancy in the direction of the two equivalent Ti neighbors along the [001] axis, whereas the neutral charge state moves toward the Ti ion in the $[1\bar{1}0]$ direction in a more symmetrical position.

This result is in contradiction to the recently published results by Yang *et al.*[11] who found that the electrons of the vacancy are shared identically with the two equivalent Ti neighbors in the [001] direction for both charge states of the vacancy. Aono *et al.*[10] reported a shf interaction for the W center in the [001] direction of about 14.7 MHz, similar to the one observed for the $S=1.0$ state of the oxygen vacancy in the same direction. It is not clear for us at the moment, if the W defect can also be interpreted in terms of a differently distorted oxygen vacancy instead of a Ti pair defect with one localized electron.

V. ENERGY LEVELS

The EPR spectra due to the oxygen vacancy in two charge states were observed in oxidized synthetic rutile samples which contain a few ppm of substitutional Fe^{3+} ions at low temperatures (<30 K) after illumination with UV and blue light. In reduced samples the same spectra of both charge states of the oxygen vacancy were also observed in dark, however, dominant EPR spectra are due to interstitial Ti^{3+}.[10] It has been assumed in literature that transition metal ions in the (3+) valence states are charge compensated by oxygen vacancies and that these vacancies are statistically distributed in the crystals[13] following the relation $2Ti_s^{4+} \leftrightarrow 2Fe_s^{3+} + V_O^{2+}$. In the case for which the transition metal ions are the dominant defects they pin the Fermi level at about 0.3 eV above the valence band.[14(a)] From our measurements, these vacancies are not observed in natural rutile crystals probably because of different charge compensation mechanism due to other substitutional transition metal ions in the (5+) valence state as for example Nb, Ta, and Mo or H^+.[14(b),17] In the first case the compensation is done when $2Ti_s^{4+} \leftrightarrow Fe_s^{3+} + Nb_s^{5+}$ and in second case when $Ti_s^{4+} \leftrightarrow Fe_s^{3+} + H_i^+$, where s and i denotes substitutional and interstitial, respectively.

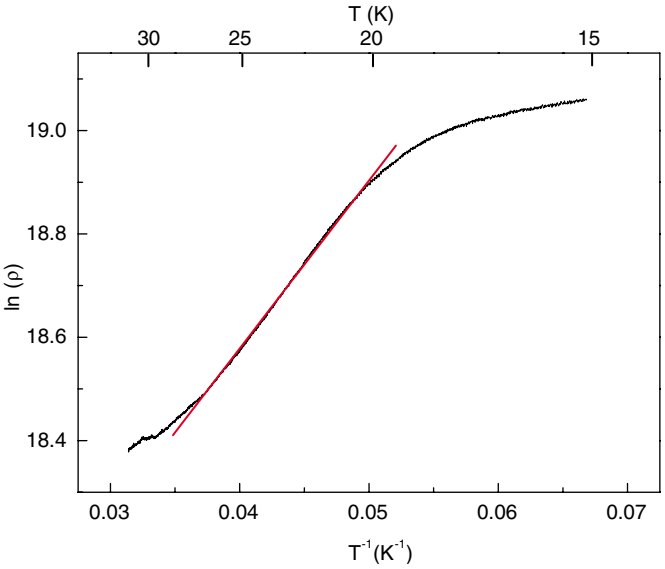

FIG. 7. (Color online) Arrhenius plot of the resistivity of oxidized TiO_2 under blue light (470 nm) in the temperature region of 15–30 K.

From our EPR measurements in the MTI synthetic rutile crystals the iron impurities, that creates an $Fe^{3+/4+}$ ionization level which pins the Fermi level at about 0.3 eV above the valence band.[14(a)] In this case, the oxygen vacancy is in the unoccupied diamagnetic charge state, V_O^{2+}. Through blue light excitation at low temperatures (<30 K) the iron impurities inject electrons into the conduction band ($Fe^{3+} + h\nu \rightarrow Fe^{4+} + e_{CB}$), which are trapped at the oxygen vacancy in two charge states, first the singly occupied state, V_O^+, and then the doubly occupied state, V_O^0, for longer illumination times (insert Fig. 2), summarizing $V_O^{2+} + e_{CB} \rightarrow V_O^+$ and $V_O^+ + e_{CB} \rightarrow V_O^0$. These trapped electrons at the vacancy states are thermally released at about 30 K (kT ~2.5 meV), suggesting a very shallow donor ionization energy level, $V_O^{+/0}$.

In order to find the energy levels associated with the oxygen vacancy, resistivity measurements in the fully oxidized sample in the 10–300 K temperature range have been performed. In dark, the resistivity is very high ($>T\Omega$) in the whole temperature range. Upon illumination with the blue LED (470 nm, 5 mW), the same as used for the EPR measurements, the conductivity increases to a more easily measurable range ($<G\Omega$). Different conductivity regimes were observed. We concentrate on the 19–27 K temperature range for which the EPR measurements have been performed. Figure 7 shows Arrhenius plot of the resistivity, $\rho = \rho_0 \exp(-\varepsilon/kT)$, as a function of the inverse temperature with ε the activation energy and k the Boltzmann constant. From that, under blue light illumination the sample shows a thermally activated regime with activation energy of 2.8 meV indicating a very shallow energy level corroborating with the conclusions drawn from the EPR measurements. It is also interesting to note that when turning off the light at 23 K, the sample shows persistent photocurrent for hours.

Recently, the singly occupied paramagnetic charge state of the oxygen vacancy in ZnO has been identified by optically detected EPR in electron irradiated ZnO at low temperatures.[18] Theoretical calculations have shown that the oxygen vacancy in ZnO is a deep donor with negative U properties, i.e., the paramagnetic charge state is metastable.[19] According to the calculations all predicted charge states suffer strong lattice relaxations and it has been concluded that the oxygen vacancy is not responsible for the *n*-type conductivity in ZnO but is a charge compensating center in *p*-type ZnO. From our experiments similar conclusions may be drawn for the oxygen vacancy in TiO_2, however, the oxygen vacancy in TiO_2 behaves as a positive U center. Theoretical calculations for different charge states of the oxygen vacancy in bulk TiO_2 are still missing.

In oxidized samples with some transition metal impurities, i.e., Fe^{3+}, Cr^{3+} and Ni^{2+}, the oxygen vacancy is responsible for charge compensation. In reduced TiO_{2-x} samples—the Fermi level is pinned by the shallow states of the Ti interstitial at about 5 meV below the conduction band as experimentally determined[20]—both charge states of the oxygen vacancy can be observed in dark, however, they are minority defects. Dominant are the titanium interstitial defects and pairs of them.[10] Theoretical calculations have shown that the oxygen vacancies may play an important role in the incorporation of magnetic transition metal ions like Co, Mn, and Fe in the TiO_2 structure[21] for application in diluted magnetic semiconductor (DMS). The magnetic ions substitute for Ti ions easier when one nearest neighbor oxygen vacancy is present with the result that the presence of the oxygen vacancy increases the magnetic moment.

VI. CONCLUSIONS

In conclusion, detailed EPR analysis of two paramagnetic charge states of the oxygen vacancy, the singly and doubly occupied states with $S=0.5$ and $S=1$, in fully oxidized rutile (TiO_2) that contain small amounts of transition metal impurities under blue light and low temperatures were presented. It was shown that both charge states present different relaxations. The oxygen vacancy is double donor, acts a compensating center for transition metal impurities and is minority defect in reduced bulk rutile, TiO_{2-x}, with gap states near the conduction band.

ACKNOWLEDGMENTS

The authors acknowledge financial supported from the Brazilian agencies FAPEMIG, CAPES, and MCT/CNPq.

*klaus@fisica.ufmg.br

[1] A. L. Linsebigler, Guangquan Lu, and John T. Yates, Jr., Chem. Rev. (Washington, D.C.) **95**, 735 (1995).
[2] A. Fujishima and K. Honda, Nature (London) **238**, 37 (1972).
[3] B. O'Reagan and M. Grätzel, Nature **353**, 135 (1991).
[4] K. D. Schierbaum, U. K. Kirner, J. F. Geiger, and W. Göpel, Sens. Actuators B **4**, 87 (1991).
[5] D. B. Strukov, G. S. Sneider, D. R. Stewart, and R. S. Williams, Nature (London) **453**, 80 (2008).
[6] R. Waser, R. Dittmann, G. Staikov, and K. Szot, Adv. Mater. (Weinheim, Ger.) **21**, 2632 (2009).
[7] G. Pacchioni, ChemPhysChem **4**, 1041 (2003); S. Wendt, P. T. Sprunger, E. Lira, G. K. H. Madsen, Z. Li, J. O. Hansen, J. Matthiesen, A. Blekinge-Rasmussen, E. Laegsgaards, B. Hammer, and F. Besenbacher, Science **320**, 1755 (2008).
[8] U. Diebold, Surf. Sci. Rep. **48**, 53 (2003).
[9] E. Cho, S. Han, H.-S. Ahn, K.-R. Lee, S. K. Kim, and C. S. Hwang, Phys. Rev. B **73**, 193202 (2006).
[10] M. Aono and R. R. Hasiguti, Phys. Rev. B **48**, 12406 (1993).
[11] S. Yang, L. E. Halliburton, A. Manivannan, P. H. Bunton, D. B. Baker, M. Klemm, S. Horn, and A. Fujishima, Appl. Phys. Lett. **94**, 162114 (2009).
[12] S. W. Hodgskiss and J. S. Thorp, J. Magn. Magn. Mater. **36**, 303 (1983).
[13] D. L. Carter and A. Okaya, Phys. Rev. **118**, 1485 (1960).
[14] M. K. Nowotny, L. R. Sheppard, T. Bak, and J. Nowotny, J. Phys. Chem. C **112**, 5275 (2008); H. J. Gerritsen and E. S. Sabisky, Phys. Rev. **125**, 1853 (1962).
[15] J. M. Spaeth and H. Overhof, *Point Defects in Semiconductors and Insulators* (Springer Verlag, Berlin, 2003).
[16] *International Tables for Crystallography*, 5th ed., edited by Theo Hahn (Kluwer, Dordrecht, 2002), Vol. A.
[17] D. C. Cronemeyer, Phys. Rev. **113**, 1222 (1959).
[18] L. S. Vlasenko and G. D. Watkins, Phys. Rev. B **71**, 125210 (2005).
[19] A. Janotti and C. G. van de Walle, Appl. Phys. Lett. **87**, 122102 (2005).
[20] E. Yagi, R. R. Hasiguti, and M. Aono, Phys. Rev. B **54**, 7945 (1996).
[21] L. A. Errico, M. Rentería, and M. Weissmann, Phys. Rev. B **72**, 184425 (2005).